

RSC Advances



This is an *Accepted Manuscript*, which has been through the Royal Society of Chemistry peer review process and has been accepted for publication.

Accepted Manuscripts are published online shortly after acceptance, before technical editing, formatting and proof reading. Using this free service, authors can make their results available to the community, in citable form, before we publish the edited article. This *Accepted Manuscript* will be replaced by the edited, formatted and paginated article as soon as this is available.

You can find more information about *Accepted Manuscripts* in the [Information for Authors](#).

Please note that technical editing may introduce minor changes to the text and/or graphics, which may alter content. The journal's standard [Terms & Conditions](#) and the [Ethical guidelines](#) still apply. In no event shall the Royal Society of Chemistry be held responsible for any errors or omissions in this *Accepted Manuscript* or any consequences arising from the use of any information it contains.



Journal Name

ARTICLE

Polyesters derived from Bio-based Eugenol and 10-Undecenoic acid: Synthesis, Characterization, and Structure-Property Relationships

Received 00th January 20xx,
Accepted 00th January 20xx

DOI: 10.1039/x0xx00000x

www.rsc.org/

Keling Hu,^a Dongping Zhao,^a Guolin Wu^{*a} and Jianbiao Ma^{*b}

Renewable monomers derived from eugenol and 10-undecenoic acid were synthesized via thiol-ene click and nucleophilic substitution reactions. With these monomers in hand, a series of thermoplastic polyesters with tunable thermo-mechanical properties were prepared via two-step melt polycondensation. The prepared polyesters exhibit weight-average molecular weights in the range of 21000-48000 g mol⁻¹, together with polydispersity values between 1.8 and 2.1. Experiments involving thermogravimetric analysis (TGA), differential scanning calorimetry (DSC) and dynamic mechanical analysis (DMA) were carried out in order to study thermal and mechanical properties of the polymers. All prepared polyester species prove to be thermally stable at temperatures up to 300 °C. Furthermore, the aromatic and semi-aromatic polyesters exhibit fully amorphous behaviours with glass transition temperatures (T_g s) ranging between -34.13 and 6.97 °C. Herein, the density of the rigid aromatic rings along the main chains of the polyester features a distinct influence on the T_g values. Furthermore, the fully aliphatic polyesters prove to be semi-crystalline with inconspicuous T_g . The incorporation of aromatic eugenol into the polyester chains and the density of the benzene rings were also found to result in a significant improvement in the mechanical properties, including Young's modulus and elongation at break in the range of 11.6 to 44.2 MPa and 33.6 to 106.7%, respectively. The relatively high $\tan \delta$ and the low storage modulus indicate that eugenol-based polyesters feature superior viscosity properties and may therefore find future applicability in a variety of high-tech materials.

Introduction

As a result of rapid depletion of fossil resources and continuously increasing environmental concerns, humanity is facing unprecedented challenges. Further emphasized by phenomena like global warming, environmental pollution and land desertification, it is urgent to find substituents of fossil energy sources.¹⁻⁵ Polyester, a type of multifunctional materials, is received an increasing demand in a multitude of industrial applications. However, most of the polyesters are currently prepared from compounds extracted from fossil feedstock. Due to decreasingly low availability of fossil resources, bio-based resources represent interesting "green" alternatives to provide the precursors needed for polyester synthesis.⁶⁻¹⁰

Amid a selection of renewable resources, plant oils,^{11, 12} including castor oil and palm oil, stand in the critically important position historically and currently due to their multifunctional transformation potential.^{13, 14} Classical and

well-established chemical transformations may preferentially be done at the ester group of the native triglycerides. Examples include hydrolysis to form free fatty acids groups and glycerol, transesterification to yield corresponding fatty acid methyl esters or hydrogenation of both fatty acids and their corresponding dimethyl esters to result in the formation of fatty alcohols. Primary oleochemicals, such as fatty acids, their corresponding methyl esters, amines and alcohols, are generally used in the production of surfactants,¹⁵ lubricants¹⁶ and coatings.^{17, 18} The use of modern synthetic techniques, together with enzymatic and microbial methods, has led to an extraordinary expansion of synthetic routes for the production of novel fatty acid compounds,¹⁹⁻²² generated from selectively modification in the alkyl chains. Due to the steric demand of the alkyl chains and the generally complex structural parameters of fatty acids, it proves to be rather tedious to obtain symmetrical diols or diesters via conventional organic synthesis. 10-Undecenoic acid, a synthetic unsaturated fatty acid derived from thermal cleavage of the naturally occurring ricinoleic acid, contains a terminal olefinic group as well as a terminal carboxylate.²³ No other functional groups or sterically demanding chains can be found, making 10-undecenoic acid an ideal candidate for the synthesis of high-purity symmetrical diesters or diols via one-step thiol-ene coupling reactions and subsequent simple recrystallization processes for purification.

^a Key Laboratory of Functional Materials, Institute of Polymer Chemistry, Nankai University, Tianjin 300071, P R China. E-mail: guolinwu@hotmail.com

^b School of Chemistry and Chemical Engineering, Tianjin University of Technology, Tianjin 300191, P R China

† Electronic Supplementary Information (ESI) available: [Additional figures]. See DOI: 10.1039/x0xx00000x

Eugenol,^{24, 25} represents a natural phenolic allylbenzene compound extracted from lignocellulosic biomass, and presents particularly in clove oil. Clove is commercially cultivated in India, Madagascar, Sri Lanka, Indonesia and the southern region in China. Eugenol is responsible for the intense aroma of cloves. The component accounts for 72%-90% of the essential oils extracted from cloves and is mainly used as an antibiotic and antihypertensive agent. Furthermore, the natural product can be used in the production of perfumes, cosmetics, soaps, and even food. In recent years, study on eugenol mainly focused on ruthenium-catalysed olefin metathesis reactions (e.g. self-metathesis,²⁶ cross-metathesis²⁷ with electron-deficient olefins) due to a terminal olefinic bond present that proves to be particularly suitable for transformations via olefin metathesis. Therefore, it may be possible to prepare different types of functionalized phenol derivatives to develop new routes for the production of different multifunctional products from renewable sources.²⁸ Noteworthy in this context is the fact that ruthenium-promoted isomerization reactions to form isoeugenol generally result in improved selectivity properties and product yields.²⁹⁻³¹ Hence, the isomerization of allylbenzenes offers an attractive synthetic approach that can be applied particularly to β -methylstyrenes, which represent common starting materials particularly in the flavour and fragrance industries, as well as valuable intermediates for the production of pharmaceutical compounds. Other than the applications listed above, *Sarojadevi* and *Thirukumar* have also discovered a novel synthetic route towards the production of polybenzoxazines via a Mannich-like condensation reaction of eugenol, formaldehyde and an amine.³² However, to the best of our knowledge, the synthesis of polyesters starting from renewable eugenol has never been reported. The terminal olefinic bond renders eugenol substrate ideal for click reactions, by which ester or hydroxyl functional groups may be incorporated. Recently, we have developed a variety of polyesters based on renewable eugenol and α,ω -diols. The polymers obtained exhibited excellent ductility.³³ Inspired by this promising result, we explored the possibility of designing polyesters from entirely renewable plant-oil sources using 10-undecenoic acid and eugenol as starting materials.

In this study, bio-based monomers derived from eugenol and 10-undecenoic acid were synthesized. The precursors **P1** and **P2** were prepared using eugenol and methyl thioglycolate or 2-mercaptoethanol via thiol-ene click reactions,³⁴⁻³⁷ followed by Williamson ether synthesis³⁸ using methyl chloroacetate or 1,4-dibromobutane to obtain the four aromatic monomers **M1-M4** were obtained. Next, methyl 10-undecenoate and 10-undecen-1-ol, derivatives of 10-undecenoic acid, were coupled with methyl thioglycolate or 2-mercaptoethanol via thiol-ene click reactions to afford the three aliphatic monomers, **M5-M7**. Using these monomers, fully aromatic polyesters, semi-aromatic polyesters and fully aliphatic polyesters were obtained via a two-step melt-polycondensation method. The influence of the aromatic eugenol incorporated into the polyester chains on the thermal and mechanical properties of the obtained polyesters was

studied and compared with the conventional fully synthetic polymers PET and PBT.

Experimental Section

Materials

Eugenol (99%), methyl thioglycolate (99%), 2-mercaptoethanol (98%), methyl chloroacetate (98%), methyl 10-undecenoate (98%), 10-undecen-1-ol (98%), tetrabutyl titanate (TBT) ($\geq 99\%$), benzoin dimethyl ether (DMPA, 99%), and ethylene carbonate (98%) were purchased from Sigma-Aldrich. 1,4-Dibromobutane (98%) and other commonly used chemical reagents were purchased from Tianjin Chemical Reagent Co. (Tianjin, China) and used without further purification. Acetonitrile, *N,N*-dimethylformamide (DMF) and other solvents were dried according to the standard methods in the literature if necessary.

Instruments and Methods

¹H NMR and ¹³C NMR spectra were recorded in CDCl₃ at room temperature using a Bruker AVANCE III 400MHz NMR spectrometer. Tetramethylsilane was used as the internal standard. Fourier transform infrared spectra (FTIR) were measured at room temperature using a Bio-Rad FTS6000 spectrophotometer. Polymer samples were prepared by grinding the polymers with KBr powder, followed by compressing the mixture to form a pellet. Fourier transform high resolution mass spectra (FTMS) were measured on a Varian 7.0T FTMS with positive electrospray ionization (+ESI). The molecular weight and polydispersity of the obtained polyesters were determined via size exclusion chromatography (SEC, Waters 1525 dual pump, Waters 2414 differential refraction detector, Waters 2487 dual UV detector and Waters 717 plus automatic sampler) at 35 °C. THF was used as the eluent at a flow rate of 1.0 mL min⁻¹. The average molecular weights were calibrated using polystyrene samples as standards. Thermogravimetric analysis (TGA) was performed using a NETZSCH TG209 analyzer. In a general method, the polymer sample was heated from 25 to 800 °C under a nitrogen atmosphere at a rate of 10 °C min⁻¹. The temperature leading to 5% weight loss, the temperature for maximum degradation rate, and residue weight (%) at 800 °C were recorded. Differential scanning calorimetric (DSC) thermograms were measured using a DSC Q100 apparatus from TA instruments. Polymer samples were first heated from 25 to 150 °C and then cooled to -80 °C. The glass transition (T_g), melting (T_m) and crystallization temperatures (T_c) and their respective enthalpies ΔH_m and ΔH_c were calculated from the second heating run. All runs were performed at a rate of 10 °C min⁻¹. The tensile assays were performed in triplicates on dog-bone-shaped sample bars (12 mm \times 2 mm \times 0.5 mm) at 25 °C at a tensile rate of 50 mm min⁻¹. Young's modulus, tensile stress at break and tensile strain at break were acquired by averaging the data from the three paralleled test specimens. Dynamic mechanical analysis (DMA) were carried out using a NETZSCH DMA242 analyzer in the controlled force-tension film mode with a preload force of 0.1 N, a deformation of 0.1%,

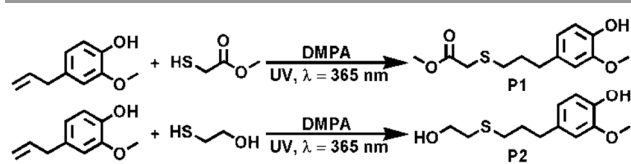
and an amplitude of 10 mm, at a fixed frequency of 1 Hz in the -60 to 60 °C range and a heating rate of 3 °C min⁻¹. The measurements were performed in triplicates using rectangular specimens (length × width × thickness = 25 × 5 × 1 mm³) obtained from casting chloroform solutions at a concentration of 0.1 g mL⁻¹.

Synthesis of precursors and monomers

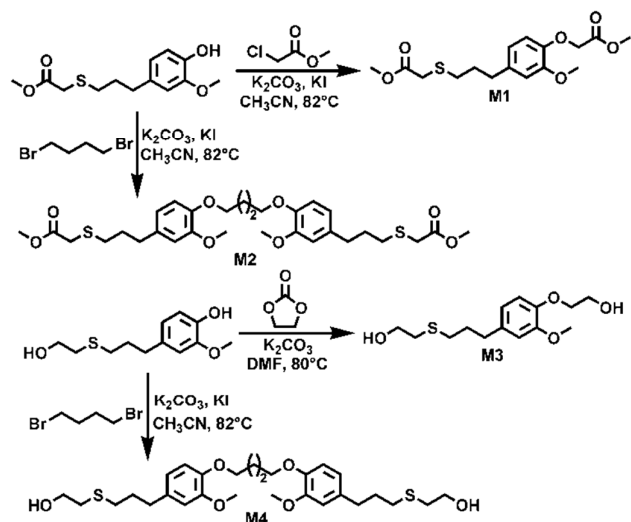
The synthetic routes of precursors, monomers are presented in Scheme 1-3. The detailed synthetic routes, characterization data and spectra are presented in the supplementary information (Experimental Section and Characterization Section, Figure S1-S13).

General procedure for the synthesis of polyesters

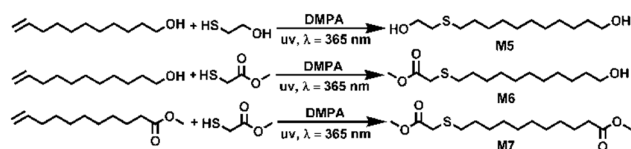
The polymerization reactions were uniformly performed in a 50 mL Schleck flask equipped with a magnetic stirrer, a nitrogen inlet and a vacuum distillation outlet. The individual reactions in this synthetic route are formulated in Scheme 4. A 1:1.05 molar ratio of diesters to diols was adopted to guarantee



Scheme 1 Synthetic routes of precursors **P1** and **P2** via thiol-ene click reactions from eugenol and mercapto-containing compounds.



Scheme 2 Synthetic routes of monomers **M1-M4** via nucleophilic substitution reactions from precursors **P1** and **P2**.

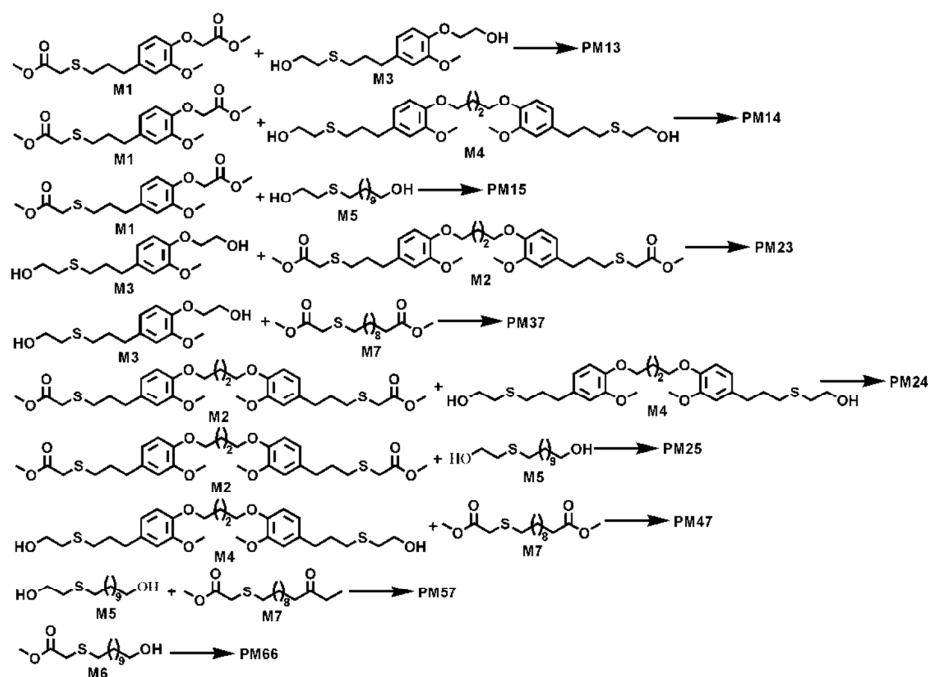


Scheme 3 Synthetic routes of monomers **M5-M7** via thiol-ene click reactions from methyl 10-undecenoate and 10-undecen-1-ol.

hydroxyl terminated. Tetrabutyl titanate (TBT, 0.6 % mmol per mol of diester) was used as the catalyst. Before transesterification, the apparatus was vented with nitrogen for 10 minutes to ensure no residual oxygen was present in the system. Transesterification reactions were carried out at 140-160 °C for about 4 hours at a low nitrogen flow. Polycondensation reactions were then conducted at 180 to 220 °C for 3-5 h under a 0.03-0.06 mbar vacuum until the viscosity of the mixture resulted in the stirrer to get stuck, indicating completeness of the reaction. The mixtures were cooled to room temperature and the atmospheric pressure was recovered with nitrogen to prevent degradation of the products. The obtained polymers were dissolved in a minimum amount of chloroform and precipitated in excess methanol, resulting in removal of any remaining oligomers and impurities formed. The product was collected by filtration and was dried in *vacuo*. **PM57** and **PM66** prove to be semi-crystalline materials, and all other polymers were found to be yellow viscous amorphous materials. The characterization data of **PM14** and **PM57** is presented below. The other obtained polymers have similar data and their corresponding spectra can be seen in Figure 1 and Figure S16-S32.

PM14. ¹H NMR (CDCl₃, 400 MHz): δ 1.84-1.93 (m, 6H, -SCH₂-CH₂-CH₂-), 1.96-2.08 (m, 4H, ArOCH₂-CH₂-), 2.51-2.60 (m, 4H, -S-CH₂-CH₂-CH₂-), 2.60-2.70 (m, 8H, -S-CH₂-CH₂-CH₂- and -SCH₂-CH₂-CH₂-), 2.71-2.80 (m, 4H, -COOCH₂-CH₂-), 3.21 (s, 2H, -S-CH₂-CO-), 3.83 (s, 6H, ArO-CH₃), 3.86 (s, 3H, ArO-CH₃), 4.02-4.12 (m, 4H, ArO-CH₂-CH₂-), 4.23-4.34 (dt, 4H, J₁ = 26.8 Hz, J₂ = 6.8 Hz, -COO-CH₂-), 4.66 (s, 3H, ArO-CH₂-CO-), 6.63-6.85 (m, 9H, Ar-H) ppm; ¹³C NMR (CDCl₃, 100.6 MHz): δ 26.06 (ArOCH₂-CH₂-), 30.29 (-SCH₂-CH₂-CH₂-), 30.35 (-SCH₂-CH₂-CH₂-), 30.53 (-SCH₂-CH₂-CH₂-), 31.27 (-S-CH₂-CH₂-CH₂-), 31.62 (-S-CH₂-CH₂-CH₂-), 31.68 (-S-CH₂-CH₂-CH₂-), 32.05 (-SCH₂-CH₂-CH₂-), 33.52 (-S-CH₂-CO-), 34.25 (-S-CH₂-CH₂-O-), 55.91 (ArO-CH₃), 55.98 (ArO-CH₃), 63.95 (-SCH₂-CH₂-O-), 64.23 (-SCH₂-CH₂-O-), 66.69 (ArO-CH₂-CO-), 68.83 (ArO-CH₂-CH₂-), 112.37 (Ar-C), 112.59 (Ar-C), 113.41 (Ar-C), 114.86 (Ar-C), 120.30 (Ar-C), 120.34 (Ar-C), 134.11 (Ar-C), 135.88 (Ar-C), 145.54 (Ar-C), 146.79 (Ar-C), 149.42 (Ar-C), 149.61 (Ar-C), 168.96 (ArOCH₂-CO-), 170.25 (-SCH₂-CO-) ppm; FTIR: 2929, 1757, 1734, 1513, 1264, 1232, 1144, 1036, 807 cm⁻¹.

PM57. ¹H NMR (CDCl₃, 400 MHz): δ 1.21-1.43 (m, 26H, -CH₂-aliphatic), 1.52-1.69 (m, 8H, -SCH₂-CH₂-CH₂-, -COOCH₂-CH₂-, and -CH₂-CH₂-CO-), 2.24-2.35 (q, J = 8.0 Hz, 2H, -CH₂-CH₂-CO-), 2.51-2.79 (m, 6H, -S-CH₂-CH₂-CH₂- and -S-CH₂-CH₂-O-), 3.18-3.25 (d, 2H, -S-CH₂-CO-), 4.01-4.16 (dt, J₁ = 6.4 Hz, J₂ = 26.4 Hz, 2H, -COO-CH₂-CH₂-CH₂-), 4.17-4.32 (dt, J₁ = 6.8 Hz, J₂ = 23.2 Hz, 2H, -COO-CH₂-CH₂-S-), ppm; ¹³C NMR (CDCl₃, 100.6 MHz): δ 24.94-25.04 (-CH₂- aliphatic), 25.88-25.96 (-CH₂- aliphatic), 28.61 (-CH₂- aliphatic), 28.70, 28.79 (-CH₂- aliphatic), 28.87 (-CH₂- aliphatic), 29.02-29.04 (-CH₂- aliphatic), 29.16 (-CH₂- aliphatic), 29.21 (-CH₂- aliphatic), 29.26 (-CH₂- aliphatic), 29.42 (-CH₂- aliphatic), 29.47 (-CH₂- aliphatic), 29.53 (-CH₂- aliphatic), 29.72 (-CH₂- aliphatic), 30.39 (-CH₂-CH₂-O-), 30.56 (-CH₂-SCH₂-CO-), 32.43 (-COOCH₂-CH₂-S-CH₂-), 32.75-32.78 (-CH₂-CH₂-CO-), 33.63-33.76 (-S-CH₂-CO-), 34.26-34.41 (-S-CH₂-CH₂-O-), 63.37 (-CH₂-O-), 64.29 (-CH₂-O-), 64.41 (-SCH₂-CH₂-O-), 65.46 (-SCH₂-CH₂-O-),



Scheme 4 Synthetic strategies of the polyesters (PM13, PM14, PM15, PM23, PM24, PM25, PM37, PM47, PM57 and PM66).

Table 1 Molecular weights, polydispersities and isolated yields of the synthesized polyesters.

Polyester	M_n (g mol ⁻¹)	M_w (g mol ⁻¹)	Polydispersity (PDI)	Isolated Yield
PM13	13000	23600	1.8	82%
PM14	11300	21600	1.9	83%
PM15	21100	41600	1.9	85%
PM23	15600	32500	2.0	83%
PM24	15900	30800	1.9	81%
PM25	23100	47600	2.0	82%
PM37	14600	28300	1.9	78%
PM47	12900	23500	1.8	80%
PM57	20700	44400	2.1	88%
PM66	21800	40900	1.8	90%

170.42 (-SCH₂-CO-), 170.72 (-SCH₂-CO-), 173.63 (-CH₂CH₂-CO-), 173.97 (-CH₂CH₂-CO-) ppm; FTIR: 2918, 1732, 1470, 1310, 1201, 1178, 992, 719 cm⁻¹.

Results and Discussion

Synthesis of precursors and monomers

Precursors P1 and P2 derived from eugenol. As a naturally occurring compound, eugenol features distinct structural characteristics. The terminal olefinic group and the phenolic hydroxyl group provide functional groups that render eugenol rather easy to derivatize. Click chemistry proposed by Sharpless in 2001,³⁴ has attracted widespread applications in organic chemistry and materials science. As the reaction procedures are usually simple to execute, highly efficient and highly selective, click chemistry provides an appealing route to heteroatom-linked molecular systems. The radical-mediated thiol-ene reaction represents one type of click reaction that is typically photo-initiated and conducted under rather mild conditions. As a consequence, sulfur-linked ester, hydroxyl and other functional groups can be introduced to the terminal olefin of eugenol in a feasible fashion. In this study, eugenol and methyl thioglycolate were reacted using DMPA and UV radiation according to a standard β -addition (Scheme 1). In the ¹H NMR spectrum of P1 (Figure S1), the appearance of two singlets at 3.2 and 3.7 ppm, one quintet at 1.8 to 1.9 ppm and the disappearance of olefinic characteristic peaks at 4.9 and 5.8 ppm, indicate the successful formation of a thioether linkage. By means of a similar protocol, 2-mercaptoethanol was unquestionably attached to the terminal olefin of eugenol (Scheme 1). The four triplets at 3.7, 2.7, 2.6 and 2.5 ppm and

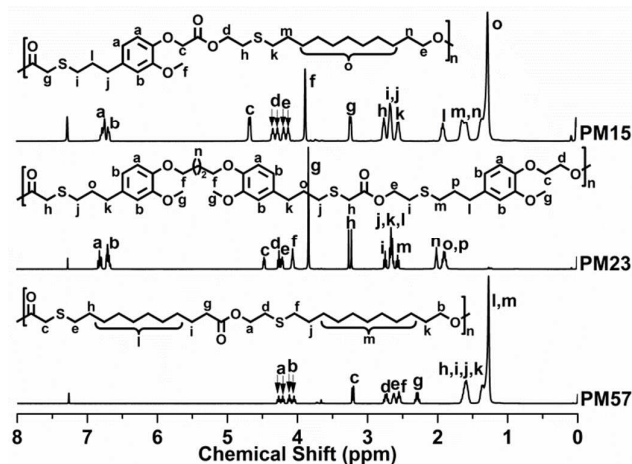


Figure 1 ¹H NMR spectra of PM15, PM23 and PM57.

one quintet at 1.8 to 1.9 ppm in the ^1H NMR spectrum of compound **P2** (Figure S1) can be clearly identified, indicating the successful formation of a thioether bond, established in a similar fashion as the β -addition in **P1**. The structures of compounds **P1** and **P2** were also confirmed by ^{13}C NMR (Figure S2 and S3) and HRMS.

Monomers **M1-M4** synthesized from precursor **P1** and **P2**.

Precursor **P1** was reacted with methyl chloroacetate to afford the asymmetrical diester monomer **M1**. As reported previously, the incorporation of phenoxy ether linkages typically increases the solubility, processability, and toughness of aromatic polymers, without compromising the thermal properties.³⁹⁻⁴¹ In order to evaluate the impact on the thermal and mechanical properties, a 1,4-dibromobutane bridged symmetrical monomer **M2** was also prepared. Monomer **M3** was prepared from **P2** and ethylene carbonate (Scheme 2). Following the same protocol of **M2**, **M4** could also be produced. The structures of **M1-M4** were all confirmed by ^1H NMR ^{13}C NMR (Figure S4-S9), FTIR and HRMS.

Monomers **M5, **M6** and **M7** prepared from methyl 10-undecenoate and 10-undecen-1-ol.** The terminal olefinic bonds render methyl 10-undecenoate and 10-undecen-1-ol ideal natural substrates for thiol-ene click chemistry. A solution of methyl 10-undecenoate and methyl thioglycolate was exposed to UV-light ($\lambda = 365$ nm) and reacted similarly to the β -addition described above (Scheme 3). The two singlets at 3.2 and 3.7 ppm in the ^1H NMR spectrum of **M7** (Figure S10) is a clear indication for a successful reaction of methyl thioglycolate with methyl 10-undecenoate. Following a similar protocol, **M5** and **M6** could be prepared. The ^1H NMR spectra of **M5** and **M6** (Figure S10) provide clear evidences for the successful synthesis. Structural parameters of **M5**, **M6** and **M7** were also obtained by ^{13}C NMR (Figure S11-S13), FTIR and HRMS.

Synthesis of polyesters

The bio-based monomers were polymerized mutually via a two-step melt-polycondensation technique to afford a series of thermoplastic polyesters as depicted in Scheme 4. TBT was used as the catalyst. The transesterification stage was carried out at 140-160°C for approximately 4 hours at a low nitrogen flow. The polycondensation reaction was then continued at temperatures ranging between 180 and 220 °C for 3-5 hours under dynamic vacuum to facilitate the removal of methanol. Upon increasing viscosity, the stirrer was found to get stuck, indicating that the polymerization reaction proceeded to completion. Noteworthy in this context is the fact that the polymerization temperature should not exceed 220 °C, since titanium alkoxides are found to decompose above this temperature, resulting in the formation of stained products. After purification, the polyesters were obtained at yields ranging between 78% and 90%. **PM66** was prepared from the self-condensation-type monomer **M6**. The stoichiometric ratio of ester and hydroxyl groups was strictly controlled to be 1:1. The molecular weights as well as polydispersities of the resulting polyesters were estimated by SEC (Figure S14 and S15). The polyesters were obtained with M_w ranging between

21600 and 47600 g mol⁻¹ and polydispersities ranging between 1.8 and 2.1 (Table 1).

The chemical compositions of the obtained polyesters could be confirmed by ^1H NMR (Figure 1, Figure S16-S18), ^{13}C NMR (Figure S19-S28) and FTIR (Figure S29-S32). From the representative ^1H NMR spectra of polyesters in Figure 1, the most obvious characteristic peaks were found between 4.1 and 4.4 ppm, corresponding to the signals for the two methylene groups adjacent to the hydroxyl group of the substrate diols being split into four triplets (**PM15** and **PM57**). However, the ^1H NMR spectrum of **PM23** features only two triplets between 4.1 and 4.4 ppm, corresponding to the two methylene groups adjacent to hydroxyl group in **M3**. This phenomenon can be ascribed to the asymmetrical nature of **M1** and **M7**, which results in the formation of two types of ester groups with different chemical environments. Meanwhile, **M2** proves to be a symmetrical diester and **M3** is determined to be an asymmetrical diol. Therefore, in the ^1H NMR spectrum of **PM23** the two methylene groups adjacent to the ester groups are split into two singlets between 3.2 to 3.3 ppm due to the asymmetrical nature of **M3**. The same feature can also be observed in the ^1H NMR spectra of **PM15** and **PM57**, where the signals for the two methylene groups adjacent to ester groups of **M1** and **M7** are uniformly split into the corresponding singlets or multiplets as a result of the asymmetrical nature of **M5**. The other polyesters exhibit similar splitting modes in their respective ^1H NMR spectrum as mentioned above. A detailed discussion on the chemical microstructures is presented in the subsequent section. This distinct difference of the ester groups in the polyesters could also be observed in the FTIR spectra. In the FTIR spectrum of **PM15** (Figure S29), two stretching vibrations of the ester carbonyl groups were observed at approximately 1734 and 1758 cm⁻¹. Meanwhile, in the FTIR spectrum of **PM23** only one stretching vibration can be found at approximately 1734 cm⁻¹.

Chemical Microstructures

The chemical microstructures of the obtained polyesters were studied using quantitative ^{13}C NMR spectroscopy. The signals of all magnetically different carbons in the polyesters can be found well resolved in the ^{13}C NMR spectra (Figure 2, Figure S33-S35). Apart from the non-protonated aromatic carbons discussed in previous reports,⁴² the carbonyl and the methylene carbons close to the asymmetrical functionalities appear to be sensitive to sequence distributions at the dyad level. As shown in Figure 2 (A) and (B), corresponding to the splitting modes of the ester carbonyls and the methylene carbon adjacent to hydroxyls of diols along the main chains of **PM15**, respectively, the resonances of all magnetically different carbon atoms present in the backbone are well resolved. Due to the unequivalence of the two ester groups in **M1** and the two methylene groups adjacent to the hydroxyl groups in **M5**, as well as the interaction between the uncoordinated esters and hydroxyl groups, four sets of dyads (**RL-RR**, **RL-RL**, **LL-RR** and **LL-RL**) with different sequence arrangements along the polyester chains were generated in **PM15**. Four methylene splitting peaks and four carbonyl splitting peaks appear in the

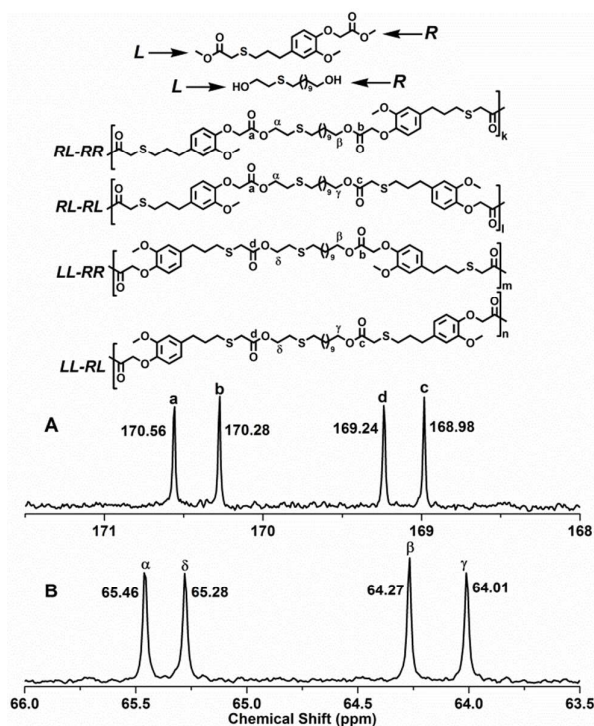


Figure 2 ^{13}C NMR signals used for the microstructure analysis of **PM15** with indication of the dyads to which they are assigned.

64–66 ppm and 168–172 ppm chemical shift regions, respectively. By integration of the four peaks, the dyad contents are found to be almost equal, which confirms the same reactivity of the participating functional groups in **M1** and **M5**. Nevertheless, **M2** features two of the same ester groups. Therefore, no splitting of the methylene carbon signals in the asymmetrical diols is observed. On the contrary, the asymmetrical methylene groups in the diols will split the ester carbonyl carbon in **M2** into two peaks (Figure S33). Furthermore, **M4** exhibits two equal hydroxyl groups equal to **M2**. It is expected that the ester carbonyls and the methylene groups adjacent to the hydroxyl groups will not split uniformly in **PM24**. According to the characteristics noted above, the chemical microstructures of the obtained polyesters can be divided into four types, *i.e.* I (**PM13**, **PM15**, **PM37** and **PM57**), II (**PM14**, **PM23**, **PM25** and **PM47**), III (**PM24**) and IV (**PM66**). Congeneric polyesters feature similar splitting modes. Therefore, the asymmetrical nature of the monomers plays a crucial role in determining the microstructures of the resulting polyesters. The ^{13}C NMR signals used for the microstructure analysis of **PM47** and **PM66** are shown in Figure S34 and S35, respectively.

Thermal Stability

The thermal stabilities of the polyesters have been comparatively investigated by TGA. The TGA and TGA derivative curves are shown in Figure 3–S36 and Figure S37–S38, respectively, and the thermal parameters are given in Table 2. The synthesized polyesters exhibit a 5% weight losses in the range of 307–351 °C. Maximum degradation rates were found

at temperatures ranging between 374 and 391 °C. The latter finding indicates a significant thermal stability, similar to commercially available polyesters. The fully aliphatic polyesters **PM57** and **PM66** were found to be more stable than the fully aromatic polyesters and the semi-aromatic polyesters. Similarly, the fully aromatic polyesters, **PM12**, **PM14**, **PM23**, and **PM34**, show comparable thermal stability as the semi-aromatic polyesters, **PM15**, **PM27**, **PM35**, and **PM47**. The relatively low thermal stability of the eugenol-based fully aromatic polyesters and the semi-aromatic polyesters is most likely attributed to the inferior structural symmetry of the monomers derived from eugenol and the presence of sulphur atoms along the polymer chains, susceptible to thermal oxidation degradation. It is well known that linear aliphatic sections can decompose almost entirely compared to aromatic sections under the same TGA conditions.⁴³ As a consequence, the fully aliphatic polyesters **PM57** and **PM66** show negligible remaining weights lower than 2% at 800 °C. Simultaneously, the eugenol-based fully aromatic polyesters and semi-aromatic polyesters feature remaining weights in the range of 6.3–17.5% at 800 °C. The increase of remaining weight may be attributed to the incorporation of aromatic benzene rings into polymer chains and the resulting reduction of aliphatic sections. All the

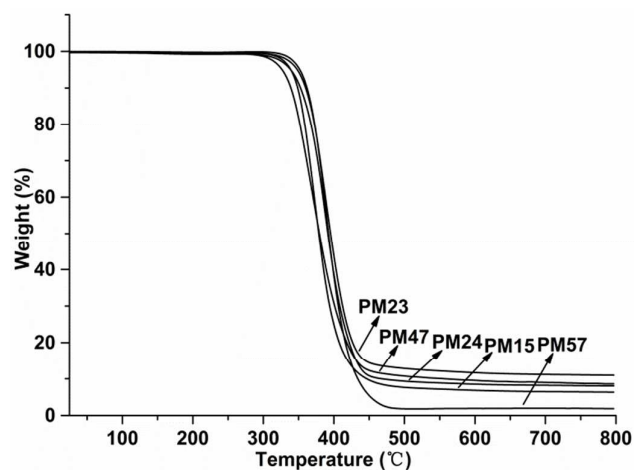


Figure 3 TGA curves of representative polyesters recorded from 25–800 °C at a heating rate of 10 °C min⁻¹ under a nitrogen atmosphere.

Table 2 Thermal properties of the synthesized polyesters.

Polymer	$T_{5\%}^a$ (°C)	T_d^b (°C)	W^c (%)
PM13	330	374	10.4
PM14	332	378	10.2
PM15	338	374	6.3
PM23	348	389	10.9
PM24	338	382	17.5
PM25	339	388	8.3
PM37	307	381	12.0
PM47	327	375	8.8
PM57	351	388	1.8
PM66	348	391	1.4

^[a] Temperature at which 5% weight loss was observed. ^[b] Temperature for maximum degradation rate. ^[c] Remaining weight at 800 °C.

polyester species exhibit a single-step degradation behaviour, indicating that the ester groups display comparable thermal stabilities both in the aliphatic and aromatic segments.

Thermo-Mechanical Properties

Important thermal properties, *i.e.* T_g , T_m , and the crystallization behaviour, were also determined by DSC. The second heating DSC curves of the polyesters without being subjected to any thermal treatments are shown in Figure 4, and the corresponding analytical data are summarized in Table 3. As can be seen from inspection of the data in Table 3, the T_g values range from -34.13 to 6.97 °C, which prove to be rather low for engineered polymers and therefore result in a rubbery material. The relatively low T_g values are most likely due to the presence of heteroatoms S and O in the scaffold, which support internal rotation characteristics of the polyester chains. Aromatic rings are known to exhibit unfavourable effects on the internal rotation and therefore lead to an enhancement of the corresponding T_g . The T_g values of the polymers in this study are closely related to the densities of aromatic rings along the polyester chains. As shown in Figure 5, the T_g values gradually increase in the range of -35-7 °C due to improving aromatic ring densities. Polyesters with the same aromatic ring densities, *e.g.* **PM15** and **PM37**; **PM25** and **PM47**; **PM14** and **PM23**, exhibit similar T_g values. The T_g of **PM24** was found to be -8.36 °C, similar to the T_g value found for **PM25** (-6.35 °C) and **PM47** (-4.05 °C). **PM24**, prepared from 1,4-dibromobutane bridged **M2** and **M4**, contains a large number of phenolic oxygens along the main chains and the rotation of C-O proceeds easier than C-C. Consequently, **PM24** exhibits a T_g close to those found for **PM25** and **PM47**. The latter finding proves to be surprising since **PM25** and **PM47** contain more aliphatic methylene groups along their corresponding chains.

From the second heating traces of DSC, it can also be observed that the fully aliphatic polyesters **PM57** and **PM66** exhibit semi-crystalline behaviours with inconspicuous T_g . All other polymer species are found to be amorphous viscous materials without fusion and crystallization characteristics. This finding is most likely due to the asymmetrical nature of

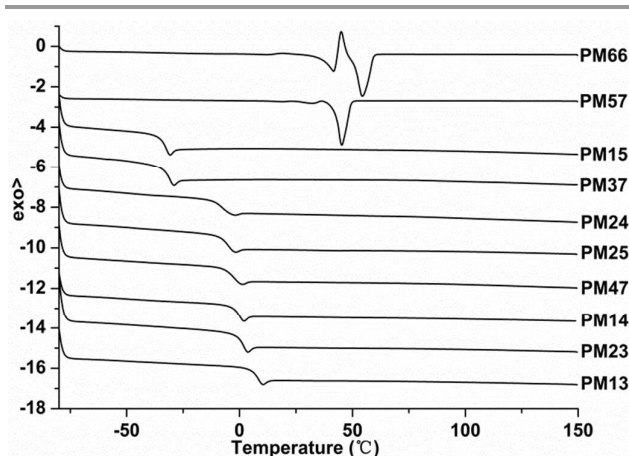


Figure 4 DSC curves of polyesters -2nd scan carried out from -80 to 150°C at a heating / cooling rate of 10°C min⁻¹.

Table 3 Melting and crystallization values obtained from -2nd DSC heating scans at a heating rate of 10°C min⁻¹.

Polymer	T_g^a (°C)	T_m^b (°C)	ΔH_m^b (J g ⁻¹)	T_c^b (°C)	ΔH_c^b (J g ⁻¹)
PM13	6.97	-	-	-	-
PM14	-1.61	-	-	-	-
PM15	-34.13	-	-	-	-
PM23	0.23	-	-	-	-
PM24	-8.36	-	-	-	-
PM25	-6.35	-	-	-	-
PM37	-32.39	-	-	-	-
PM47	-4.05	-	-	-	-
PM57	-	45.35	80.06	30.13	76.82
PM66	-	$T_{m1} = 41.66$	$\Delta H_{m1} = 24.82$	28.56	98.74
		$T_{m2} = 54.83$	$\Delta H_{m2} = 81.98$		

[a] Glass transition temperature measured by DSC during the -2nd heating scan at 10°C min⁻¹. [b] Melting (T_m) and crystallization (T_c) temperature and their respective enthalpies (ΔH_m , ΔH_c) measured by DSC at a heating / cooling rate of 10°C min⁻¹.

M1 and **M2**. The presence of methoxy groups adjacent to the phenyl rings in **M1** and **M2** increases the structural asymmetry further, and the incorporation of long-chain linear aliphatic diols into the polyester chains cannot compensate for these structural defects. Therefore, random polyesters derived from renewable eugenol seem to be unfavourable for the regular packing of crystalline chains.

Tensile Properties

To evaluate the influence of the eugenol-based monomers on the mechanical properties, tensile assays were carried out using films that were prepared via casting from chloroform solutions. Due to the relative brittleness exhibited by **PM57** and **PM66**, films of these polymers could not be prepared. The majority of the other polymer species were found to be in an amorphous state caused by the lack of symmetry and the low T_g values (-34.13 for **PM15** to 6.97°C). As a consequence, we have only been able to produce fashioned films of polymers **PM13**, **PM14**, **PM23** and **PM47** and the tensile assays were carried out thereafter. The stress-strain curves recorded from essayed polyesters are shown in Figure 5 and the mechanical parameters measured are illustrated in Table 4. The stress-strain curves demonstrate that the mechanical properties of eugenol-based fully aromatic polyesters prove to be far superior compared to the semi-aromatic polyesters. The Young's modulus ranging from 11.61 to 44.23 MPa were found to increase with the density of rigid phenyl rings incorporated into the polyester backbones. **PM13**, prepared from single aromatic **M1** and **M3**, features the highest aromatic rings density compared to other polyesters and therefore exhibits the maximal Young's modulus. **PM47**, prepared from 1,4-dibromobutane bridged **M4** and aliphatic **M7**, features the smallest number of aromatic rings and the most methylene units along the polyester chains. As a consequence, the smallest Young's modulus is observed. Unfortunately, the values of Young's modulus observed are most likely not high enough for potential application as structural materials compared to conventional PET (M_w : 32100, PDI: 2.5)⁴⁴ and

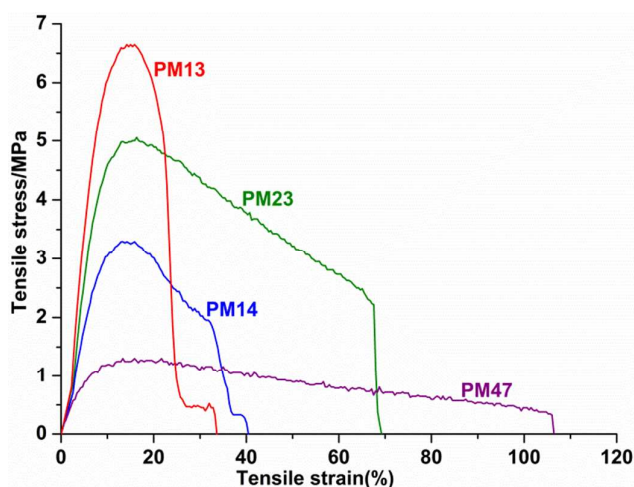


Figure 5 Stress-strain curves of polyesters at 20°C, 50 mm min⁻¹.

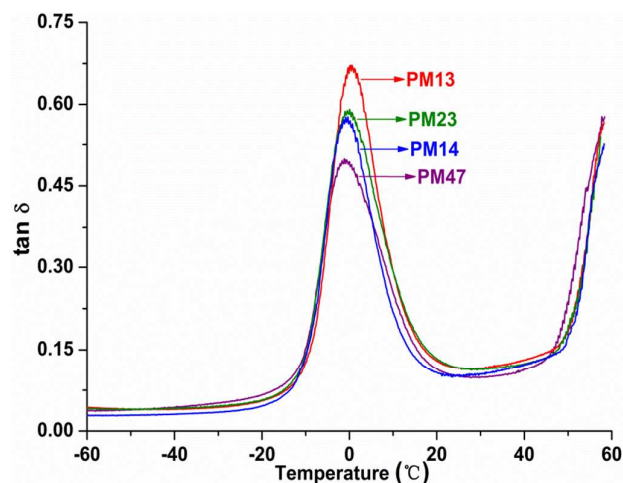


Figure 6 Tan δ as a function of temperature for PM13, PM14, PM23 and PM47.

Table 4 Tensile properties of the synthesized polyesters.

Polymer	Young's modulus (MPa)	Ultimate strength (MPa)	Elongation at break (%)
PM13	44.2 ± 4.8	0.3 ± 0.1	33.6 ± 4.2
PM14	24.7 ± 1.5	0.3 ± 0.1	40.5 ± 2.8
PM23	31.0 ± 2.4	2.2 ± 0.5	68.8 ± 3.6
PM47	11.6 ± 4.8	0.3 ± 0.1	106.7 ± 4.2
PET	1032 ± 52	45 ± 7	23 ± 5
PBT	841 ± 15	42 ± 5	14 ± 3

PBT (M_w : 41300, PDI : 2.4).⁴⁵ The presence of methoxy groups adjacent to the phenoxy groups reduces the structural symmetry and crystallinity so that the mechanical strength of the polyesters is reduced accordingly. The elongation at break ranging from 33.64–106.67% displays an opposite effect. The semi-aromatic polyester **PM47** features a maximal elongation at break of 106.67%, while the fully aromatic polyester **PM13** exhibits an elongation at break of 33.64%. The higher elongations at break indicate that eugenol-based polyesters exhibit excellent ductility characteristics. Although PET and PBT feature higher modulus and strength properties, the elongations at break found are significantly lower (*i.e.* 14% to 23%). It has already been demonstrated that PET or PBT materials without any additives prove to be rather brittle. Plasticizers are usually added to increase structural integrity of PET or PBT materials in an effort to meet strict engineering standards set by the polymer industry in the production of synthetic polymers. Copolymerization with monomers derived from renewable eugenol may therefore offer an innovative approach to increase the structural toughness of PET and PBT.

Dynamic mechanical analysis

In order to evaluate the viscoelasticity of the synthesized polyesters and to further understand the structure-property relationships, dynamic mechanical analyses (DMA) of the polyesters were carried out. The T_g values are adopted as the inflection temperature points of the maximum in loss modulus (E'').⁴⁶ As noted above, all polyesters exhibit common glass transitions temperatures, except for the fully aliphatic species **PM57** and **PM66**. However, DMA provided more conclusive

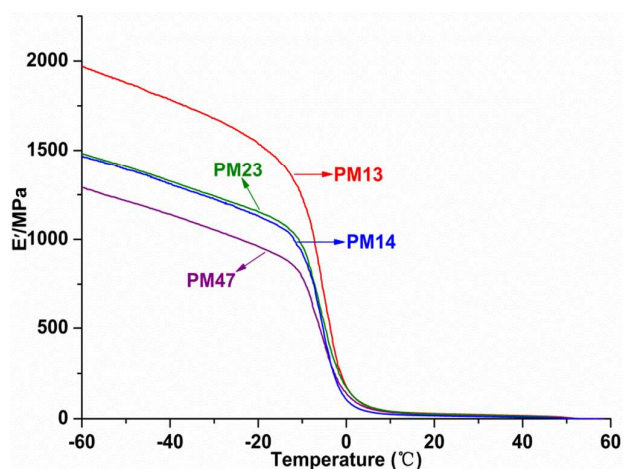


Figure 7 Storage modulus (E') as a function of temperature for PM13, PM14, PM23 and PM47.

Table 5 Dynamic mechanical properties of PM13, PM14, PM23 and PM47

Polymer	T_g (°C)	$E'(20^\circ\text{C})$ (MPa)	$\tan \delta_{\text{max}}$
PM13	0.63	124.70	0.67
PM14	-0.33	110.77	0.55
PM23	0.06	52.54	0.57
PM47	-1.16	69.17	0.48

results. As for **PM23**, T_g was determined from the loss modulus versus temperature trace (Figure S39) to be approximately 0.06 °C. The latter value is almost comparable to the value obtained by DSC (*i.e.* 0.23 °C). The other three polyester species features similar results, with the T_g values being in close agreement with the DSC results obtained. Regarding the hysteresis loss $\tan \delta$, the value is closely related to the molecular structures (*i.e.* the density of aromatic rings). As mentioned above, the fully aromatic **PM13**, **PM14** and **PM23** feature higher aromatic ring densities compared the semi-aromatic species **PM47**. When the polyesters are subjected to alternative forces or strains, the internal friction resistances observed are found to be in the following order: **PM13** > **PM14** \approx **PM23** > **PM47**. The $\tan \delta$ value gradually increases in a

similar fashion as the internal friction resistance (Figure 6), as well as the loss modulus. On the contrary, the storage modulus values adopt an adverse trend of $\tan \delta$ (Figure 7). According to the data listed in Table 5, the $\tan \delta_{\max}$ values are found to be higher than the one observed for vanillic acid-polyesters previously reported by our group.⁴⁷ On the other hand, the storage moduli are found to be rather lower, indicating that the eugenol-based polyesters presented here feature superior viscosity properties. Therefore, such materials may be able to absorb more impact energy and may potentially be utilized as high impact materials or toughening additives of conventional engineering plastics, e.g. PET and PBT, to increase structural integrity.

Conclusions

In an effort to fully or partially replace petroleum-based resources using renewable biomass in the industrial production of polyesters, a feasible method for monomer synthesis from renewable eugenol and 10-undecenoic acid has been developed. Furthermore, a series of thermoplastic polyesters were prepared from these renewable monomers via two-step melt polycondensation. The chemical structures and compositions were confirmed by ¹H NMR, ¹³C NMR and FTIR spectroscopy. Results from thermogravimetric analyses show that all the prepared polyester species exhibit superior thermal stabilities at temperature up to 300 °C, comparable with the commercially available structural materials PET and PBT. Differential scanning calorimetry results demonstrate that the fully aromatic and semi-aromatic polyesters feature amorphous behaviours, with T_g values ranging from -34.13 to 6.97 °C. This finding indicates that the methoxy group adjacent to the phenolic hydroxyl group significantly impedes the structural symmetry. The fully aliphatic polyesters exhibit semi-crystalline behaviours, with discreet T_g values. The density of the rigid benzene rings along the polyester chains was also found to influence T_g . The stress-strain and dynamic mechanical analysis results reveal that the Young's modulus and ultimate strength are not particularly high. However, the ductility of the polyesters was found to be superior. The elongations at break reach values up to 106.7%, and the relatively high $\tan \delta$ and the low storage modulus provide a clear indication for eugenol-based polyesters featuring superior viscosity properties. In addition, the tensile properties (Young's modulus, ultimate strength and elongations at break) and dynamic mechanical properties (storage modulus and $\tan \delta$) are also closely related to the density of the aromatic rings. While some properties of the polymers obtained remain to be improved and further studies addressing these concerns are currently underway, implementation of such improvements may lead to materials incorporating eugenol-based polymers with potential applications in high impact rubbery-type materials or as additives in conventional engineered polymers designed to increase structural integrity.

Acknowledgement

This work was funded by NSFC (51203079), the Natural Science Foundation of Tianjin (14JCYBJC18100), and PCSIRT (IRT1257).

References

1. A. Corma, S. Iborra and A. Velty, *Chem Rev*, 2007, **107**, 2411-2502.
2. B. Kamm, *Angew Chem Int Edit*, 2007, **46**, 5056-5058.
3. P. N. R. Vennestrom, C. M. Osmundsen, C. H. Christensen and E. Taarning, *Angew Chem Int Edit*, 2011, **50**, 10502-10509.
4. C. H. Christensen, J. Rass-Hansen, C. C. Marsden, E. Taarning and K. Egeblad, *Chemsuschem*, 2008, **1**, 283-289.
5. A. L. Marshall and P. J. Alaimo, *Chem-Eur J*, 2010, **16**, 4970-4980.
6. G. Q. Chen and M. K. Patel, *Chem Rev*, 2012, **112**, 2082-2099.
7. R. A. Sheldon, *Green Chem*, 2014, **16**, 950-963.
8. A. Gandini, *Green Chem*, 2011, **13**, 1061-1083.
9. A. Gandini, *Macromolecules*, 2008, **41**, 9491-9504.
10. C. Vilela, A. F. Sousa, A. C. Fonseca, A. C. Serra, J. F. J. Coelho, C. S. R. Freire and A. J. D. Silvestre, *Polym Chem-Uk*, 2014, **5**, 3119-3141.
11. M. A. R. Meier, J. O. Metzger and U. S. Schubert, *Chem Soc Rev*, 2007, **36**, 1788-1802.
12. U. Biermann, U. Bornscheuer, M. A. R. Meier, J. O. Metzger and H. J. Schafer, *Angew Chem Int Edit*, 2011, **50**, 3854-3871.
13. U. Biermann, W. Friedt, S. Lang, W. Luhs, G. Machmuller, J. O. Metzger, M. R. Klaas, H. J. Schafer and M. P. Schneider, *Angew Chem Int Edit*, 2000, **39**, 2206-2224.
14. P. Gallezot, *Chem Soc Rev*, 2012, **41**, 1538-1558.
15. P. Foley, A. K. Pour, E. S. Beach and J. B. Zimmerman, *Chem Soc Rev*, 2012, **41**, 1499-1518.
16. R. Garces, E. Martinez-Force and J. J. Sales, *Grasas Aceites*, 2011, **62**, 21-28.
17. B. A. J. Noordover, A. Heise, P. Malanowski, D. Senatore, M. Mak, L. Molhoek, R. Duchateau, C. E. Koning and R. A. T. M. van Benthem, *Prog Org Coat*, 2009, **65**, 187-196.
18. C. Gioia, M. Vannini, P. Marchese, A. Minesso, R. Cavalieri, M. Colonna and A. Celli, *Green Chem*, 2014, **16**, 1807-1815.
19. G. Q. Chen, *Chem Soc Rev*, 2009, **38**, 2434-2446.
20. W. H. Lu, J. E. Ness, W. C. Xie, X. Y. Zhang, J. Minshull and R. A. Gross, *J Am Chem Soc*, 2010, **132**, 15451-15455.
21. J. W. Song, E. Y. Jeon, D. H. Song, H. Y. Jang, U. T. Bornscheuer, D. K. Oh and J. B. Park, *Angew Chem Int Edit*, 2013, **52**, 2534-2537.
22. C. Aouf, E. Durand, J. Lecomte, M. C. Figueroa-Espinoza, E. Dubreucq, H. Fulcrand and P. Villeneuve, *Green Chem*, 2014, **16**, 1740-1754.
23. M. Van der Steen and C. V. Stevens, *Chemsuschem*, 2009, **2**, 692-713.
24. J. Zakzeski, P. C. A. Bruijninx, A. L. Jongerius and B. M. Weckhuysen, *Chem Rev*, 2010, **110**, 3552-3599.
25. J. A. M. Lummiss, K. C. Oliveira, A. M. T. Pranckevicius, A. G. Santos, E. N. dos Santos and D. E. Fogg, *J Am Chem Soc*, 2012, **134**, 18889-18891.
26. D. F. Taber and K. J. Frankowski, *J Org Chem*, 2003, **68**, 6047-6048.

ARTICLE

Journal Name

27. J. Moise, S. Arseniyadis and J. Cossy, *Org Lett*, 2007, **9**, 1695-1698.
28. H. Bilel, N. Hamdi, F. Zagrouba, C. Fischmeister and C. Bruneau, *Rsc Adv*, 2012, **2**, 9584-9589.
29. C. R. Larsen and D. B. Grotjahn, *J Am Chem Soc*, 2012, **134**, 10357-10360.
30. B. Lastra-Barreira and P. Crochet, *Green Chem*, 2010, **12**, 1311-1314.
31. B. Lastra-Barreira, A. E. Diaz-Alvarez, L. Menendez-Rodriguez and P. Crochet, *Rsc Adv*, 2013, **3**, 19985-19990.
32. P. Thirukumaran, A. Shakila and S. Muthusamy, *Rsc Adv*, 2014, **4**, 7959-7966.
33. K. L. Hu, D. P. Zhao, G. L. Wu and J. B. Ma, *Polym Chem-Uk*, 2015, Doi 10.1039/c5py01075f.
34. H. C. Kolb, M. G. Finn and K. B. Sharpless, *Angew Chem Int Edit*, 2001, **40**, 2004-2021.
35. C. E. Hoyle and C. N. Bowman, *Angew Chem Int Edit*, 2010, **49**, 1540-1573.
36. C. E. Hoyle, A. B. Lowe and C. N. Bowman, *Chem Soc Rev*, 2010, **39**, 1355-1387.
37. A. B. Lowe, *Polym Chem-Uk*, 2014, **5**, 4820-4870.
38. E. Fuhrmann and J. Talbiersky, *Org Process Res Dev*, 2005, **9**, 206-211.
39. G. P. Yu, C. Liu, J. Y. Wang, T. S. Gu and X. G. Jian, *Polym Degrad Stabil*, 2009, **94**, 1053-1060.
40. M. Zaheer and R. Kempe, *Acs Catal*, 2015, **5**, 1675-1684.
41. M. R. Sturgeon, S. Kim, K. Lawrence, R. S. Paton, S. C. Chmely, M. Nimlos, T. D. Foust and G. T. Beckham, *Acs Sustain Chem Eng*, 2014, **2**, 472-485.
42. C. Lavilla, E. Gubbels, A. Alla, A. M. de Ilarduya, B. A. J. Noordover, C. E. Koning and S. Munoz-Guerra, *Green Chem*, 2014, **16**, 1789-1798.
43. J. Wu, P. Eduard, L. Jasinska-Walc, A. Rozanski, B. A. J. Noordover, D. S. van Es and C. E. Koning, *Macromolecules*, 2013, **46**, 384-394.
44. C. Japu, A. M. de Ilarduya, A. Alla, M. G. Garcia-Martin, J. A. Galbis and S. Munoz-Guerra, *Polym Chem-Uk*, 2013, **4**, 3524-3536.
45. C. Lavilla, A. M. de Ilarduya, A. Alla, M. G. Garcia-Martin, J. A. Galbis and S. Munoz-Guerra, *Macromolecules*, 2012, **45**, 8257-8266.
46. F. Stempfle, B. S. Ritter, R. Mulhaupt and S. Mecking, *Green Chem*, 2014, **16**, 2008-2014.
47. C. C. Pang, J. Zhang, G. L. Wu, Y. N. Wang, H. Gao and J. B. Ma, *Polym Chem-Uk*, 2014, **5**, 2843-2853.